

EVALUATION OF THE FREE JET SPREADING RATE PARAMETER  
FOR AXI-SYMMETRIC FLOW OF AIR AT MACH NUMBER THREE

By

CLIFFORD C. CHRISMAN

Bachelor of Science

Bradley University

Peoria, Illinois

1956

Submitted to the faculty of the Graduate School of  
the Oklahoma State University  
in partial fulfillment of the requirements  
for the degree of  
MASTER OF SCIENCE  
August, 1962

Thesis

1962

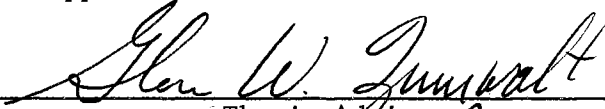
CSSA

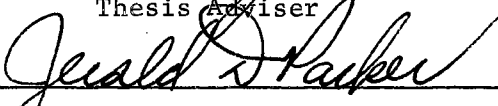
copy 2


NOV 7 1962

EVALUATION OF THE FREE JET SPREADING RATE PARAMETER  
FOR AXI-SYMMETRIC FLOW OF AIR AT MACH NUMBER THREE

Thesis Approved:

  
\_\_\_\_\_  
Thesis Adviser

  
\_\_\_\_\_  
Dean of the Graduate School

  
\_\_\_\_\_  
Dean of the Graduate School

504366

## ACKNOWLEDGEMENT

The author wishes to express his gratitude to the educational staff of the Mechanical Engineering Department at Oklahoma State University. The author is particular indebted to his adviser, Dr. Glen W. Zumwalt, for his guidance and inspiration during the accomplishment of this thesis. Dr. Zumwalt is an individual who truly excels in his field. Further indebtedness is due the personnel of the Mechanical Engineering Laboratory for their aid in the construction of the experimental apparatus. Also, a word of commendation is due Mrs. Claudine King for her excellent typing and proof-reading of this manuscript. The author wishes to express his appreciation to the United States Air Force for making his advanced study possible, and finally, to his wife, Reta, for her patience, encouragement, and sacrifice during the preparation of this thesis.

## TABLE OF CONTENTS

Chapter	Page
I. INTRODUCTION . . . . .	1
II. THEORY . . . . .	3
A. Physical Description of Turbulent Free Jet Mixing. . . . .	3
B. Analysis of the Velocity Profile of a Free Jet Mixing Region. . . . .	4
C. Evaluation of Spreading Parameter Constant. . . . .	6
D. Published Values of the Free Jet Spreading Parameter . . . . .	8
III. DESCRIPTION OF APPARATUS . . . . .	10
A. Supersonic Axi-Symmetric Nozzle . . . . .	10
B. Free Jet Mixing Chamber . . . . .	11
C. Self-ejecting Supersonic Diffuser . . . . .	11
D. Instrumentation for Pressure Probe. . . . .	13
IV. EXPERIMENTAL PROCEDURE . . . . .	15
V. METHOD OF CALCULATION. . . . .	17
VI. RESULTS AND ANALYSIS OF TEST DATA. . . . .	19
VII. CONCLUSIONS AND RECOMMENDATIONS. . . . .	21
SELECTED BIBLIOGRAPHY . . . . .	35
APPENDIX. . . . .	37

## LIST OF FIGURES

Figure	Page
A. Two-Dimensional Compressible Free Jet . . . . .	4
B. Determination of the Jet Spreading Parameter, $\sigma$ , from the Velocity Profile . . . . .	7
C. Boundary Layer Correction . . . . .	20
1. Dimensionless Velocity Profiles for Mach Number 3 . . . . .	23
2. Jet Spreading Rate Parameter Versus Mach Number . . . . .	24
3. Inverse Jet Spreading Rate Parameter Versus Mach Number . . . . .	25
4. Variation of $\sigma$ with Dimensionless Distance. . . . .	26
5. $\sigma$ Values for Mach Number 3 with Attempted Boundary Layer Correction . . . . .	27
6. Advancing Mechanism and Pressure Probe. . . . .	28
7. Supersonic Diffuser . . . . .	29
8. Testing Unit. . . . .	30
9. Nozzle Exit Pressure Profile. . . . .	31
10. Experimental Apparatus. . . . .	32
11. Control Panel . . . . .	33
12. Mixing Chamber. . . . .	34

## NOMENCLATURE

b	Width of mixing region
c	An empirical constant
c*	Speed of sound at Mach one
C	Crocco number
D	Diameter
k	Specific heat ratio
l	Prandtl's mixing length
M	Mach number
M*	Ratio of flow velocity to velocity at sonic conditions
P <sub>x</sub>	Static pressure before shock
P <sub>0x</sub>	Stagnation pressure before shock
P <sub>0y</sub>	Stagnation pressure after shock
t	Time
u	Velocity in flow direction in mixing region
U	Free stream velocity
v	Velocity in transverse direction in mixing region
x, y	Cartesian coordinates

## Greek Letters

$\beta$	Dummy variable
$\delta$	Boundary layer thickness
$\epsilon$	Virtual kinematic viscosity
$\eta$	Position parameter

$\rho$	Density
$\sigma$	Free jet spreading rate parameter
$\tau$	Viscous shearing stress
$\phi$	Dimensionless velocity

#### Subscripts

x	Before shock
y	After shock
o	Stagnation condition
$\infty$	Free stream condition

#### Superscripts

*	References to sonic conditions
---	--------------------------------



## CHAPTER I

### INTRODUCTION

Little is known experimentally or theoretically about the basic phenomena of gas in the mixing region of a supersonic axi-symmetric free jet with turbulence. Considerable theoretical and experimental work has been done in the past on free jet mixing but principally for two-dimensional (plane) constant pressure flow. The free jet must vary from free stream velocity ( $U_{\infty}$ ) at the inside edge of the mixing region to zero velocity at the outside edge. Experimental work on free jet mixing is still needed for determining the rate of spread of the mixing region. This spreading rate constant ( $\sigma$ ) is used in missile base pressure calculations, in ejector calculations, and in rocket exhaust flow problems.  $\sigma$  is the only experimental information required by the well known mixing theory of Korst (1)<sup>1</sup>. Values of  $\sigma$  as a function of Mach number are currently based on very meager data, and this principally for plane flow, the most reliable probably being that given by Liepmann and Laufer (2). A straight line approximation of  $\sigma$  versus Mach number is commonly used by extending a straight line from Tollmein's (3) value ( $\sigma = 12$  at  $M = 0$ ) through a grouping of experimentally determined values of  $\sigma$  near  $M = 1.6$  which vary from 15 to 17. (See Figure 2).

In connection with contract work being performed for the Sandia

---

<sup>1</sup> ( ) Refers to Selected Bibliography.

Corporation on non-steady, axi-symmetric base pressure problems, more exact knowledge of  $\sigma$  values became imperative. Sandia agreed to run velocity profiles on axi-symmetric free jets exhausting into the atmosphere at Mach numbers of 0.70, 0.85, 0.95, 1.50, and 2.00.  $M = 2$  requires a supply pressure of about eight atmospheres to produce the desired free jet. Above this Mach number, the ratio of supply pressure to jet pressure rises rapidly, becoming about 37:1 at  $M = 3$ . To obtain data at higher Mach numbers, Oklahoma State University agreed to develop a constant pressure axi-symmetric free jet in a low pressure mixing chamber. The free jet was to be several diameters long with  $M = 3$ . Values of  $\sigma$  at various axial stations from the nozzle exit were to be determined. These data were to be correlated with those supplied by the Sandia Corporation.

The purpose of this thesis was to design and develop a self-ejecting free jet chamber and to determine the value of  $\sigma$  for the axi-symmetric free jet at a value of  $M = 3$ . In the testing, the stagnation temperature of the free jet was equal to that of the surrounding air. Measurements of total pressure were taken by moving a pressure probe across the mixing zone at various axial stations from the nozzle exit, i.e., the point where the mixing of the free jet with the still air first occurs. From these pressure readings, assuming negligible static pressure gradient across the mixing zone, the velocity variation across the mixing zone was determined. These data provided the necessary information for the calculation of the spreading parameter  $\sigma$ . A full description of the experimental apparatus is given, together with the resulting velocity profiles and calculated values of the spreading parameter.

## CHAPTER II

### THEORY

#### A. Physical Description of Turbulent Free Jet Mixing

Axi-symmetric turbulent free jet mixing occurs very frequently and greatly affects the adjacent flow field. A few examples of this type of flow are:

1. Flow past the blunt base of a projectile.
2. Jet flow at the base of a missile.
3. Separated flow inside an over-expanded nozzle.
4. Flow resulting from the sudden expansion of a round duct.

Situations often exist in which combinations of the above are involved, especially 1 with 2 or 3. The distinguishing property of free turbulent jets is the absence of solid flow boundaries and hence the absence of a laminar sub-layer. A free jet boundary occurs between two streams moving at different velocities in the same direction. Such a surface of discontinuity in the velocity of flow is unstable and gives rise to a zone of turbulent mixing downstream of the point where the two streams first meet. The width of this mixing region increases linearly with  $x$  for plane jet flow,  $x$  being the streamwise distance from the point where the free jet mixing starts. The free jet spreads out and its average velocity decreases, but the total momentum remains constant. It has been found that the rate of spread of the mixing region for a supersonic free jet is less than the rate of spread of a subsonic

free jet (i.e.,  $\sigma$  is larger). A short distance downstream of the mixing region, the original boundary layer loses its identity; and the flow results only from the occurrence of the mixing region, the undisturbed free jet, and still air.

An important occurrence of free jet mixing is that resulting from a sudden recession of a guiding wall, resulting in a downstream facing surface, referred to as a "base." In subsonic flow, the pressure at the base of a sudden enlargement is about equal to the pressure of the entering jet. For supersonic velocities, immediately downstream of the sudden enlargement, the base pressure is generally quite different from the pressure of the entering jet. Mixing theories exist which have proven useful in calculating the base pressure of a missile. An improper calculation could cause an error in design resulting in the recirculation of hot nozzle exhaust gases back toward the base which in turn could cause a failure of the missile. This problem is greatly magnified on missiles with multiple nozzles arranged in a circular pattern.

To obtain a physical understanding of the spreading rate parameter, first consider compressible flow over a suddenly recessed plane wall.

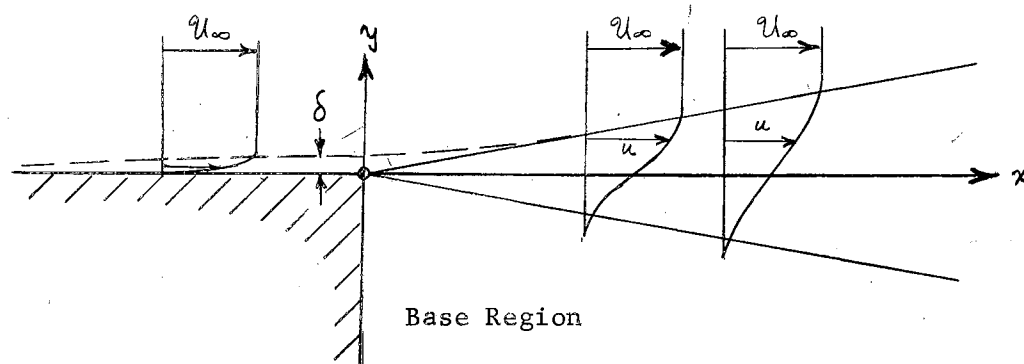


Figure A. Two-Dimensional Compressible Free Jet.

Along the mixing region, a short distance downstream of the corner, the velocity profile becomes fully developed. (See Figure A.) This means that the velocity profiles at different distances  $x$  can be made congruent by a suitable choice of a width scale factor. The velocity in the mixing region is now a function of only one variable which is defined as  $\eta = \sigma y/x$ , the position parameter. A rough estimate of the distance for the velocity profile to become fully developed is ten boundary layer thicknesses. (3).

#### B. Analysis of the Velocity Profile of a Free Jet Mixing Region

By simplifying assumptions, such as negligible static pressure gradient in the transverse direction, it is permissible to study free jet mixing problems with the aid of the two-dimensional plane boundary layer equations:

$$1) \text{ Equation of Motion: } \frac{\partial u}{\partial t} + u \frac{\partial u}{\partial x} + v \frac{\partial u}{\partial y} = \frac{1}{\rho} \frac{\partial \tau}{\partial y}$$

$$2) \text{ Continuity Equation: } \frac{\partial u}{\partial x} + \frac{\partial v}{\partial y} = 0$$

Consider the case where two streams whose constant velocities are  $U_\infty$  and  $U'_\infty$ , respectively, where  $U_\infty > U'_\infty$ . Downstream of the point of encounter ( $x = 0$ ), the streams will form a mixing region. The first solution to the problem under consideration was given by Tollmien (3), for plane, laminar, incompressible jet mixing. He made use of Prandtl's mixing length hypothesis for turbulent shear.

$$3) \tau = \rho l^2 \left| \frac{\partial u}{\partial y} \right| \frac{\partial u}{\partial y}$$

Goertler (4) arrived at a simpler solution by using Prandtl's hypothesis for the shearing stress.

$$4) \tau = \rho \epsilon \frac{\partial u}{\partial y}$$

$$5) \epsilon = c b (u'_\infty - u_\infty)$$

Here, virtual kinematic viscosity is assumed constant over the entire width of the mixing region and approximately constant in the x-direction.

The incompressible solution obtained by Goertler was

$$6) \quad u = \frac{u_{\infty} + u'_{\infty}}{2} \left\{ 1 + \frac{u_{\infty} - u'_{\infty}}{u_{\infty} + u'_{\infty}} \operatorname{erf} \eta \right\},$$

where  $\sigma = \eta y/x$  and

$$7) \quad \operatorname{erf} \eta = \frac{2}{\sqrt{\pi}} \int_0^{\eta} e^{-\beta^2} d\beta.$$

If  $u'_{\infty} = 0$ , the above equation reduces to

$$8) \quad \frac{u}{u_{\infty}} = \frac{1}{2} (1 + \operatorname{erf} \eta)$$

Substituting for  $\operatorname{erf} \eta$  and letting  $\phi = \frac{u}{u_{\infty}}$  one obtains

$$9) \quad \phi = \frac{1}{2} + \frac{1}{\sqrt{\pi}} \int_0^{\sigma \frac{y}{x}} e^{-\beta^2} d\beta.$$

For compressible turbulent flow, equation 8) has been shown by Korst (1) to be valid but now  $\sigma$  is a function of Mach number. This equation can also be used for axi-symmetric compressible flow providing the radius is large compared to the width of the mixing region.

### C. Evaluation of Spreading Parameter Constant ( $\sigma$ ).

Evaluation of  $\sigma$  may be performed from considering the slope at the inflection point in the velocity profile. For

$$\phi = \frac{1}{2} \left[ 1 + \operatorname{erf} \left( \sigma \frac{y}{x} \right) \right],$$

$$\frac{d\phi}{dy} = \frac{1}{\sqrt{\pi}} e^{-(\sigma y/x)^2} \left( \frac{\sigma}{x} \right), \text{ and}$$

$$10) \quad \frac{d^2\phi}{dy^2} = \frac{2y\sigma^3}{x^3\sqrt{\pi}} e^{-(\sigma y/x)^2} = 0.$$

Thus, the inflection point occurs when  $y = 0$ , and the slope of the curve at  $y = 0$  is

$$11) \left( \frac{d\phi}{dy} \right)_{y=0} = \frac{1}{\sqrt{\pi}} \frac{\sigma}{x} .$$

Solving for  $\sigma$ :

$$12) \sigma = x \sqrt{\pi} \left( \frac{d\phi}{dy} \right)_{y=0}$$

$\left( \frac{d\phi}{dy} \right)_{y=0}$  can be approximated by drawing a tangent to the experimentally determined curve of  $u/U_\infty$  versus  $y/x$  at  $y = 0$  and  $u/U_\infty = 0.5$ . By Figure B, it is easily seen that  $\left( \frac{d\phi}{dy} \right)_{y=0} \approx \frac{\Delta\phi}{\Delta y} \approx \frac{1}{2y_j}$ .

Thus; 
$$13) \sigma = \frac{x \sqrt{\pi}}{2 y_j}$$

This method is acceptable in principle; but in practice, this is not the most accurate method. A more accurate method is described later.

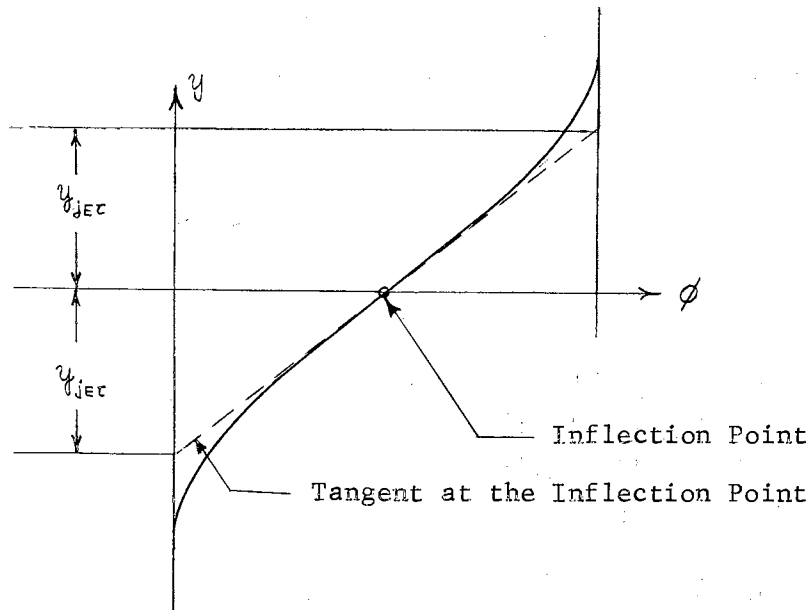


Figure B. Determination of the Jet Spreading Parameter,  $\sigma$ , from the Velocity Profile.

#### D. Published Values of the Jet Spreading Parameter

Tollmien (3) considered the mixing of an incompressible, two-dimensional free jet at constant velocity with the adjacent still air. As previously mentioned, Tollmien discovered that the plot of dimensionless velocity ( $u/U_\infty$ ) versus dimensionless distance ( $\sigma y/x$ ) closely approximates a Gaussian error function, where  $\sigma$  is the calculated value that will fit the experimental measurements to the error function. Tollmien's value of  $\sigma$  was found to be 12. Liepmann (2) determined experimentally the velocity distribution in the mixing region and the rate of spread, both into the jet and into the surrounding air, for a two-dimensional incompressible jet. He verified Tollmien's spreading rate parameter value of  $\sigma = 12$ . Abramovich (6) developed the theory of free turbulence propagation and boundary layer theory for a plane-parallel free subsonic jet in which the compressibility effects were included. No  $\sigma$  determination was reported. Gooderum (7) presented the results of the mixing of a two-dimensional supersonic free jet of  $M = 1.6$  and  $\rho_{jet} = 1.5 \rho_{still\ air}$  by measuring the density variations by an interferometer across the mixing zone in the region near the nozzle. The experimentally determined value of the spreading rate parameter was found to be 15. Pai (8) determined that for turbulent jet mixing in two-dimensional compressible flow of  $M = 1.7$  that  $\sigma = 17$ . Pai worked with a rectangular jet exhausting into the atmosphere. Two other values for  $\sigma$  were obtained at the University of Maryland in 1954 by an optical study of two-dimensional jet mixing at  $M = 1.6$  and 1.8. (9). For both Mach numbers,  $\sigma$  was 17.2.

Four scattered data points existing for the spreading rate parameter for compressible flow are shown in Figure 2. These values were all



determined for the same Mach number range and only for two-dimensional flow. Tripp (10) suggested using a straight line approximation of  $\sigma$  versus Mach number by extending a straight line from Tollmien's value through this scattered grouping of experimentally determined values of  $\sigma$ . (See Figure 2.)  $\sigma$  was thus approximated by  $\sigma = 12 + 2.758M$ . Although this linear equation for  $\sigma$  is based upon very meager data, it is being widely used. Goethert (11) used this linear formula for  $\sigma$  in his recent article on base flow on missiles with clustered rockets, even though the Mach number was well above that of the existing data points and the nozzles were axi-symmetric.

## CHAPTER III

### DESCRIPTION OF APPARATUS

As explained previously, it was required to produce a shock free, unbounded jet for axi-symmetric compressible flow. One requirement was that the exit pressure of the nozzle be the same as the pressure of the media into which the compressible jet was flowing. Supply stagnation pressure to the nozzle was not sufficient to satisfy this requirement for  $M = 3$ , the Mach number desired for the tests, with flow into the atmosphere. Thus, exit pressure being less than atmospheric pressure, it was necessary to exhaust the nozzle into a low pressure area. Rather than produce this low pressure area with a vacuum pump, it was decided that the same effect could be produced by a self-ejecting supersonic diffuser. Therefore, design components consisted of:

- A. Supersonic axi-symmetric nozzle
  - B. Free jet mixing chamber
  - C. Self-ejecting supersonic diffuser (ejector)
  - D. Instrumentation for pressure probe
- A. Design of the Axi-symmetric Supersonic Nozzle

In order to generate a uniform, shock-free jet, one must maintain a uniform profile at the nozzle exit. The nozzle must be carefully designed since uniform flow fields are not easily produced. The nozzle was designed by the Foelsch (12) method with a throat diameter of

0.55 inches, an exit diameter of 1.132 inches, and a design Mach number of three. Nozzle contour dimensions are given in Appendix A, along with the design equations used. The nozzle was constructed of brass with no allowance made for the thickness of the boundary layer since the total length of the nozzle was quite small. The nozzle was operated with high pressure, dried, cooled air supplied to a large plenum chamber in which the stagnation pressure level was controlled. The nozzle exit velocity profile was checked for uniformity by measuring the pressure variation across the flow at the exit. The resulting uniform pressure profile is shown in Figure 9.

#### B. Free Jet Mixing Chamber

The mixing chamber or vacuum chamber was designed from a 12-inch long, 1/4-inch wall thickness, 6-inch outside diameter cylindrical section of lucite. Lucite was chosen to enable an observer to see inside the mixing chamber during tests. Initial tests of the mixing chamber showed that it would not withstand the high compressive forces produced by the vacuum (about -11 psig) without dangerous deformation. This problem was solved by putting a reinforcing ring around the outside of the mixing chamber. This kept the cross-section of the chamber circular and enabled it to withstand the large compressive forces. The ring also provided a very adequate guide for the pressure probe. A diagram of the mixing chamber is shown in Figure 8.

#### C. Self-Ejecting Supersonic Diffuser

The design of the ejector was the most critical. This unit keeps the pressure of the mixing chamber equal to that of the exhausting jet

which is a necessary condition to maintain the desired supersonic axisymmetric free jet. An ejector that is too efficient will produce a chamber pressure lower than the nozzle exit pressure resulting in an under-expanded nozzle. Similarly, an ejector with too low an efficiency will result in an over-expanded nozzle since the nozzle exit pressure will be less than the chamber pressure. The ejector was designed so that it could be moved from a position just downstream of the nozzle exit to its operating position several diameters downstream of the nozzle exit. The final ejector designed was constructed of a straight section of  $1\frac{1}{4}$  inch diameter standard steel pipe followed by an aluminum expansion section. The expansion section had a  $4\frac{1}{2}$  degree divergence angle and a 3.47:1 exit to inlet area ratio. (See Figure 7.)

The major problem encountered while designing the ejector was that of maintaining supersonic flow with the ejector inlet several diameters downstream of the nozzle exit. Several different designs were tried before satisfactory results were obtained. The first ejector consisted of only a straight 12-inch section of  $1\frac{1}{4}$  inch diameter standard steel pipe. This ejector produced a strong shock in the exit portion of the nozzle causing subsonic flow in the mixing chamber. An expansion cone with an exit to inlet area ratio of four and a six-degree divergence angle was added to this straight section. A test then showed that this unit was also unsatisfactory. Next, the ejector was modified from a fixed position type to a variable type in hopes that one could "pick up" the shock near the nozzle and obtain supersonic flow in the mixing region by slowly backing the ejector away from the nozzle to its operating position. After several design attempts with unsatisfactory results, Kline's (13) article on optimum design of

straight walled diffusers was consulted, and the final workable design for the expansion cone obtained.

The inlet diameter of the ejector was determined by estimating  $\eta$  of the streamline (j) which defines the mass flow from the nozzle. Calculating  $\sigma$  from the approximate linear formula  $\sigma = 12 + 2.758M$ , and knowing the desired operating position  $x$ , the inlet diameter of the ejector was calculated from the formula  $D = 0.55 + 2(x)\left(\frac{\eta}{\sigma}\right)$ . To obtain  $\eta$ ,  $\phi$  was obtained for  $M = 3$  from a chart of  $\phi$  vs  $C^2$ . (1).  $C^2$  was calculated from the formula  $C^2 = \frac{M^2}{\frac{2}{k-1} + M^2} = \frac{9}{5+9} = 0.643$  which in turn gave  $\phi_j = 0.670$ .

Thus,  $\phi = 0.670 = \frac{1}{2} (1 + \text{erf } \eta)$ ,

and  $\eta = 0.311$ .

Therefore,  $D = 1.132 + 2(8) \left(\frac{0.311}{20.27}\right) = 1.38$  inches.

This method gave a very good initial estimate of the necessary size of the inlet diameter. By trial and error, the diameter that gave satisfactory results was found to be a slightly larger one of 1.50 inches.

#### D. Instrumentation for Pressure Probe

By considering the static pressure constant across the mixing region, one need only measure the existing static pressure in the mixing chamber and the total pressure variation across the mixing region to determine the velocity profile. Thus, the instrumentation consisted of a total pressure probe constructed from 0.039-inch diameter stainless steel hypodermic tubing mounted on a 1/8 inch diameter brass rod. The hypodermic tubing was mounted transverse to the flow stream. The end of the tubing was sealed and a .0071-inch diameter hole

drilled in the side of the tube. The tube was oriented such that the hole faced upstream, and was then advanced along its own axis. (See Figures 6 and 8.) This was the third probe design used. The first was a pitot-static probe mounted in a brass wedge. This probe proved to be too large, resulting in a strong shock pattern which destroyed the supersonic free jet mixing region. The second probe was an L-shaped total pressure probe that was also unsatisfactory since drag caused it to bend and turn giving erroneous data.

The total pressure probe was mounted through a hole drilled in the wall of the lucite mixing chamber and advanced across the mixing region by means of a threaded, hand-advanced, mechanical pusher. One-quarter turn of the pusher advanced the probe  $1/96$ th of an inch into the mixing region. Static pressures were taken at the nozzle exit, at the mixing chamber wall, and from the total pressure probe before it entered the mixing region. (See Figure 8.) All pressures were recorded from readings on mercury manometers.

## CHAPTER IV

### EXPERIMENTAL PROCEDURE

The experimental investigation was performed on a plenum chamber (Figure 10) operated by a 170 horsepower natural gas engine that drove a two-stage compressor. The speed of the power unit which controlled plenum chamber pressure was regulated remotely from the control panel (Figure 11) by air. All tests were performed at Mach numbers of approximately three. The power unit was started and time allowed for plenum chamber pressure to stabilize at the desired operating pressure. Reference readings of the mercury manometers and barometric pressure were recorded before each test run. The flow system and pressure lines were checked for leaks and instruments inspected to insure proper operation. A zero reference reading was taken before advancing the probe into the mixing region. The plenum chamber pressure was adjusted to make the three static pressure readings as close as possible insuring a uniform velocity profile in the test region. The total pressure probe was then advanced across the mixing region by means of the hand-operated advancing mechanism. (See Figure 6.) One full turn of the advancing mechanism advanced the total pressure probe  $\frac{4}{96}$ ths of an inch into the mixing region (in the y-direction). Between advancements of the probe, approximately two minutes were allowed for stabilization. Total pressure readings were taken from a point outside the mixing region to the axis of the axi-symmetric flow so that the uniformity of the velocity

profile could be checked. Since there was only a small difference between the mixing region temperature and room temperature, it was assumed that adiabatic flow existed. Velocity profiles were measured from axial station ( $x = 0$ ) to axial station ( $x = 4.625$  inches) which was just a little over eight radii from the nozzle exit. Lack of a higher plenum chamber pressure prevented velocity profile measurements at larger axial stations.



## CHAPTER V

### METHOD OF CALCULATION

A pressure probe inserted into a supersonic flow produces a shock wave at the upstream side of the probe. Thus, the total pressure recorded in the supersonic portion of the mixing region was the stagnation pressure, ( $p_{0y}$ ), just downstream of a normal shock wave. In the subsonic portion, there is no shock wave produced by the probe so that supply total pressure is obtained. The ratio of the static pressure before the shock ( $p_x$ ) to the total pressure after the shock ( $p_{0y}$ ) gave  $M^*$ , defined as the ratio of  $u/c^*$ .  $M^*_{\infty}$  was calculated from the measured total pressure of the free stream.  $M^*_{\infty}$  was cross-checked by another pressure ratio of static pressure to plenum chamber pressure  $\frac{p_x}{p_{0x}}$ . For each position  $y$  of the total pressure probe, a corresponding value of  $u/U_{\infty}$  was determined giving the mixing region velocity profile which was made dimensionless by plotting  $u/U_{\infty}$  versus  $y/x$ . The  $y/x = 0$  axis was shifted to coincide with the portion of the curve where  $u/U_{\infty} = 0.5$ . Thus, a new plot  $u/U_{\infty}$  versus  $y'/x$  was obtained. This was necessary since  $\eta = \sigma y/x$  is only true when coordinates are such that  $\eta = 0$  when  $\phi = 0.5$ .  $\sigma$  was now calculated for each position  $y'/x$  by determining the corresponding value of  $\eta$  from measured  $\phi$ ,  $y/x$ , and the previously derived equation  $\phi = 1/2 + 1/2 \operatorname{erf} \eta$ . This method is more practical than the method described in part 3 of the theory providing that  $\eta$  is only calculated for  $\phi$  values in the

ranges  $\phi = 0.15$  to  $\phi = 0.45$  and  $\phi = 0.55$  to  $\phi = 0.85$ . When  $\phi$  is between 0.45 and 0.55, both  $\eta$  and  $y/x$  are very small. Therefore, small errors in  $\phi$  or  $y/x$  can produce large errors in  $\sigma$ . When  $\phi$  is less than 0.15 and greater than 0.85, small changes in  $\eta$  result in very large changes in  $y'/x$  which again may result in poor values of  $\sigma$ .

The average value of  $\sigma$  for  $\eta$  in the range 0.15 to 0.45 and 0.55 to 0.85 was determined by this method for axial station  $x = 1.44, 2.219, 3.347, 4.625$  inches.

## CHAPTER VI

### RESULTS AND ANALYSIS OF THE TEST DATA

A total of ten runs were made at five axial stations. A plot of these data ( $\sigma$  versus  $y'/x$ ) is shown in Figure 1. From these data, a value of  $\sigma$  for each axial station was computed. A plot of  $\sigma$  versus  $x/R$  is shown in Figure 4. Also included in this plot are  $\sigma$  values obtained from the Sandia Corporation tests at  $M = 0.70, 0.85, 0.95, 1.5,$  and  $2.0$ . It is evident that  $\sigma$  increases from axial station zero until the boundary layer effect is damped out and then stabilizes at a relatively constant value. Actually,  $\sigma$  values for low  $x/R$  have little meaning since the assumed error function profile had not yet developed from the boundary layer shape.  $\sigma$  values from O.S.U. tests at axial stations near the nozzle do not follow the same trend as Sandia Corporation values at the lower Mach numbers. This may be due to the magnified boundary layer effect of the higher speed. The dashed line in Figure 4 indicates the actual  $\sigma$  variation expected at  $M = 3$ .

An axial station large enough to produce a mixing region width of the same order of magnitude as the radius of the exhausting jet was desired but was not obtained due to insufficient plenum chamber pressure. However, it is believed that when this happens, the  $\sigma$  value will start to decrease. An indication of this is shown in Figure 4. To verify this phenomenon, the Sandia Corporation will later run axial stations  $x/R$  of 12 and 16 at  $M = 1.5$  and  $M = 2.0$ . A plot of  $\sigma$  versus

Mach number utilizing previously published results and the results of this experimental analysis, along with that of Sandia, is shown in Figure 2. These data points indicate that  $\sigma$  is not a linear function of Mach number as previously assumed by Tripp but is almost constant for the incompressible range ( $M = 0.7$ ) and then a quickly increasing function of Mach number. A plot of  $\sigma$  versus Mach number (Figure 3) more clearly shows the trend of the spreading rate parameter for the free jet as  $M$  is increased.

A correction for the initial boundary layer thickness was attempted by extrapolating selected  $\phi$  lines on profiles at two axial stations to the apparent origin of the linearly spreading mixing region. The  $\Delta x$  correction was determined to be approximately 1.38 inches. Using this,

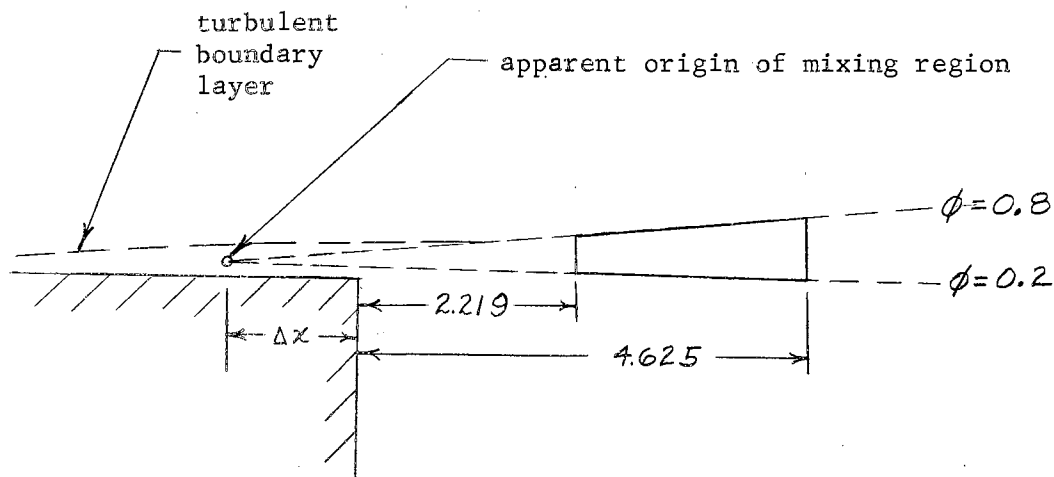


Figure C. Boundary Layer Correction.

corrected values of  $\sigma$  were computed. These are shown in Figure 5. These values are not believed to be very accurate since the axial stations used were close together and the divergence angle was small. Thus, a small error in  $y/x$  could cause a very large error in the corrected  $x$  distance. It may be noted that previous investigators performed no such correction.

## CHAPTER VII

### CONCLUSIONS AND RECOMMENDATIONS

Test data show that Tripp's approximated linear formula for  $\sigma$  is not as accurate as current usage of the spreading rate parameter requires. The  $\sigma$  values arrived at in this thesis, correlated with Sandia Corporation data, indicate that  $\sigma$  values for Mach numbers less than 1.6 are actually smaller than those obtained by Tripp's linear formula,  $\sigma = 12 + 2.758M$ , while  $\sigma$  values for Mach numbers greater than 1.6 are actually larger than those obtained by Tripp's formula. Figure 1 shows the dimensionless velocity profiles. The boundary layer effect can be seen for axial stations near the nozzle; namely,  $x/R = 3.920$  and  $x/R = 2.544$ . Figure 2 shows the variation of  $\sigma$  with Mach number. The constancy of  $\sigma$  for subsonic flow was not anticipated, but is reasonable if one recalls that compressibility effects are negligible below  $M = 0.7$ . Figure 3 shows the inverse jet spreading parameter versus Mach number. Note that  $(1/\sigma)$  seems to become asymptotic to 0 at high Mach numbers. Figure 4 shows the variation of  $\sigma$  with dimensionless distance from the nozzle.

Recommendations for further experimental investigations are:

1. Evaluation of  $\sigma$  for higher Mach numbers.
2. Evaluation of  $\sigma$  at sufficient distances from the nozzle so that the axi-symmetric effect may be studied, i.e., at a distance that is large enough for the width of the mixing region

to be of the same order of magnitude as the radius of the nozzle. This is to be accomplished for  $M = 1.5$  and  $M = 2.0$  by the Sandia Corporation, with  $x/R$  of about 12 to 16.

3. Values of  $\sigma$  exist only for turbulent mixing. Chapman (14) shows that a different fully-developed profile exists for laminar mixing for which  $\sigma$  values are unknown. Values of  $\sigma$  for this type of flow at high Mach numbers may be needed in the near future since laminar separated boundary layers become more stable at hypersonic conditions.

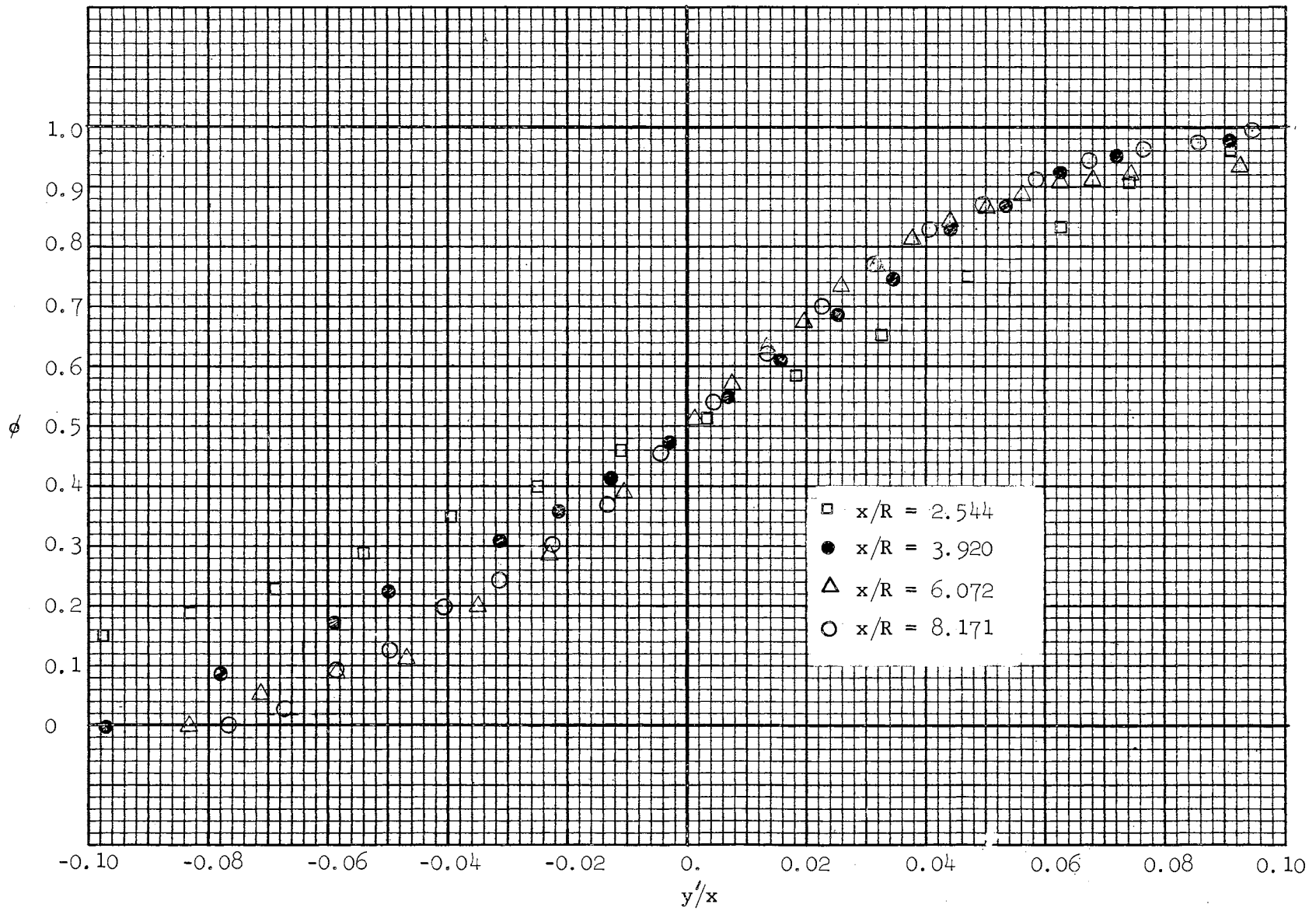


Figure 1. Dimensionless Velocity Profiles for Mach Number 3.

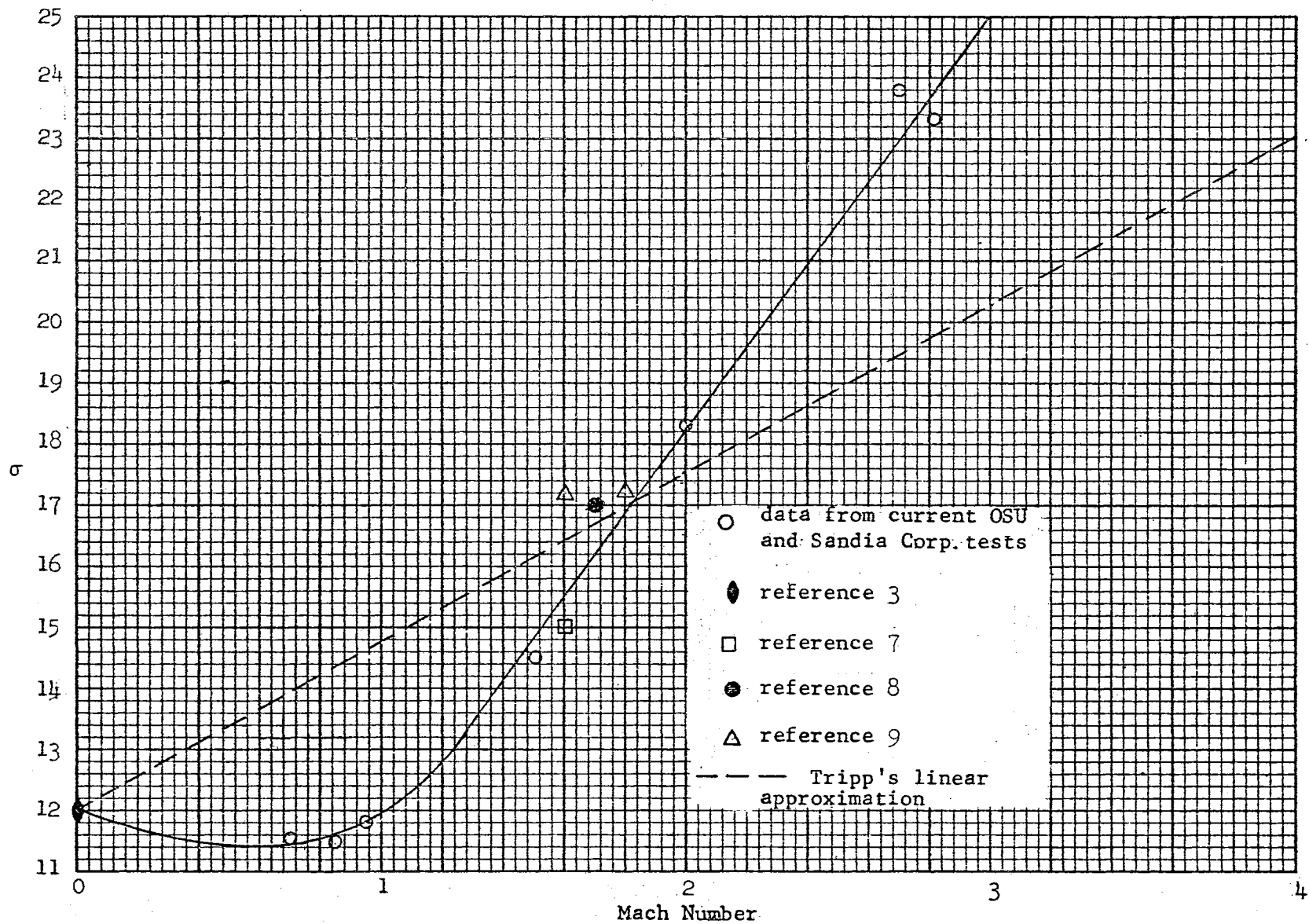


Figure 2. Jet Spreading Rate Parameter Versus Mach Number.



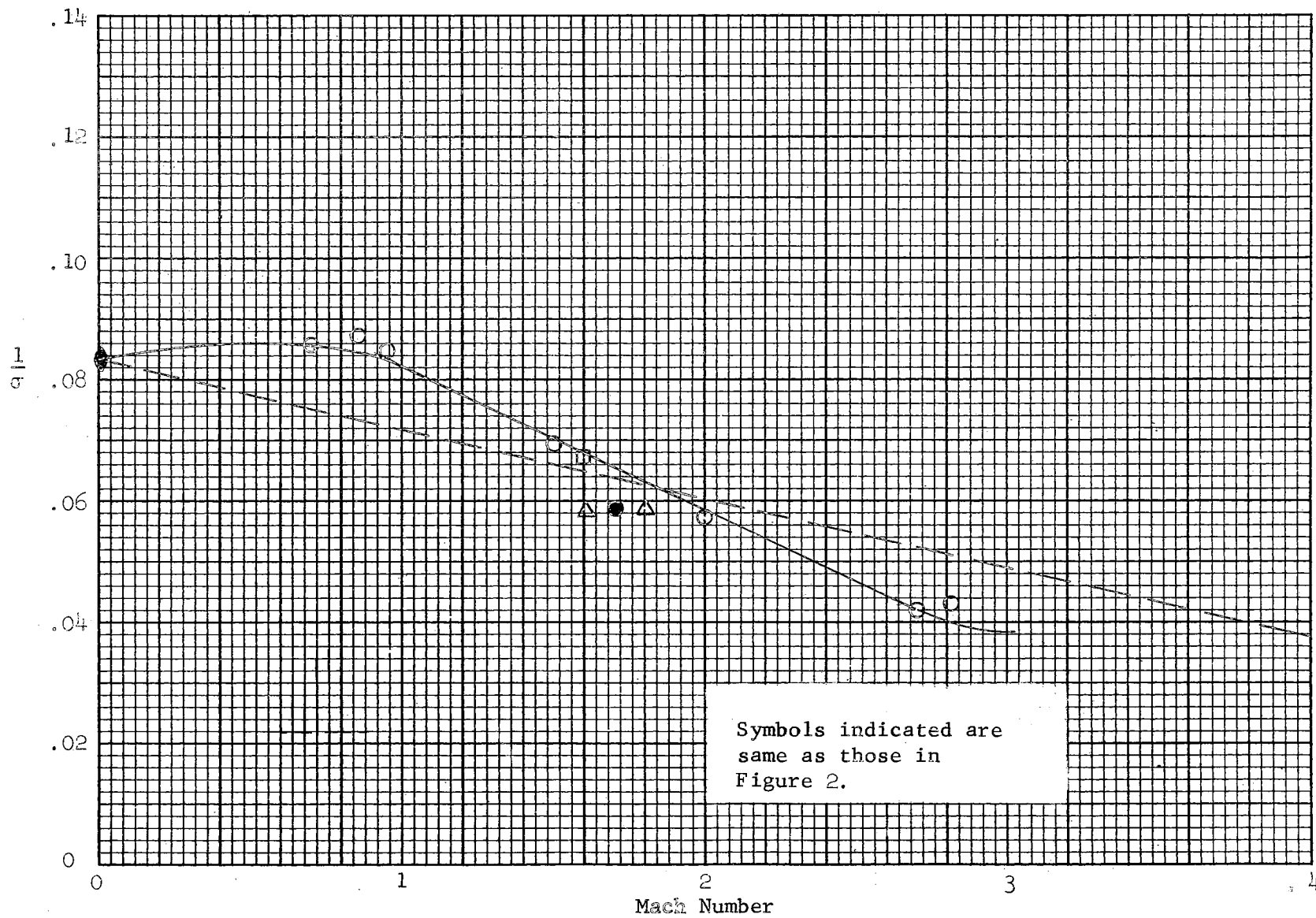


Figure 3. Inverse Jet Spreading Rate Parameter Versus Mach Number.

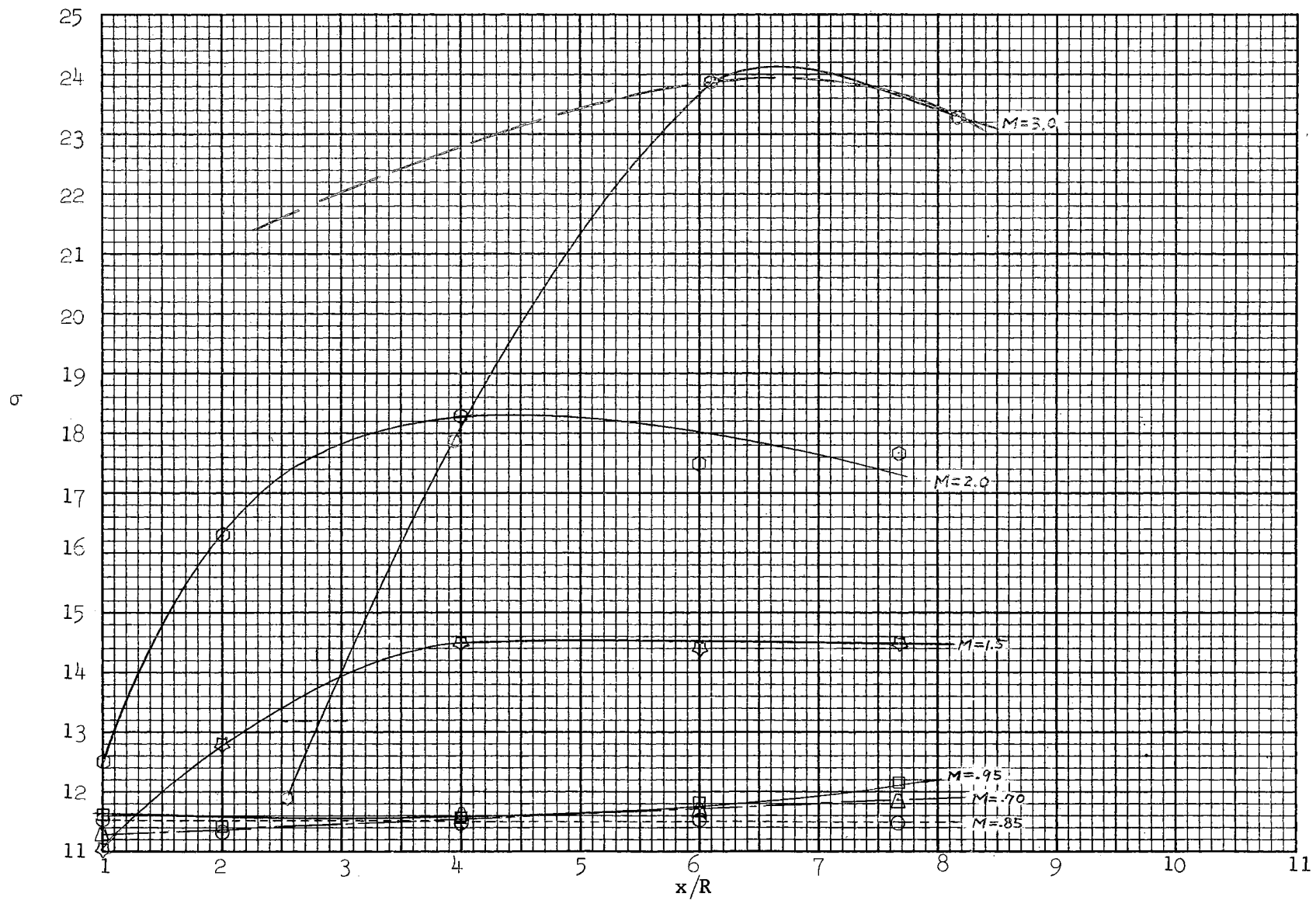


Figure 4. Variation of  $\sigma$  with Dimensionless Distance.

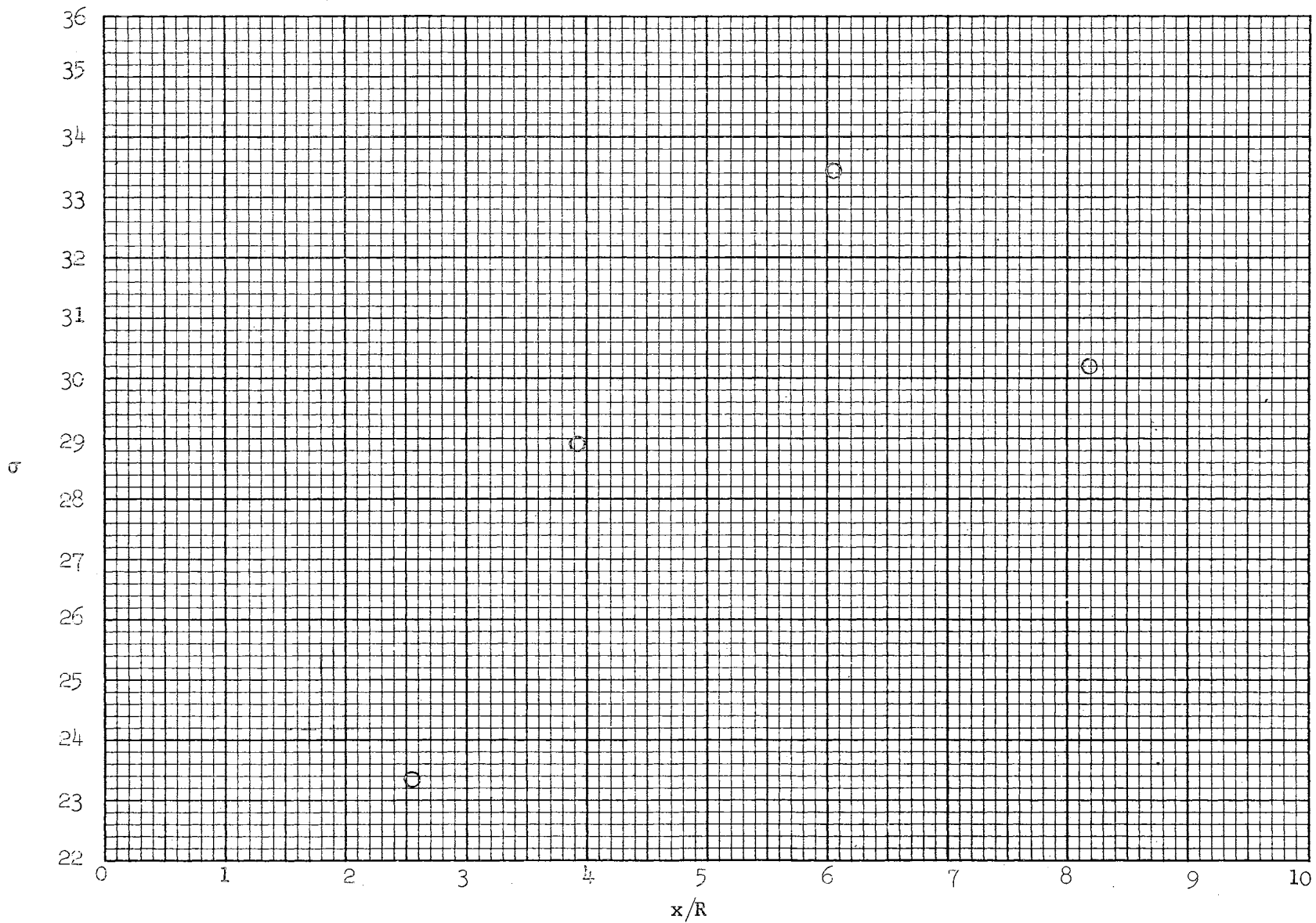
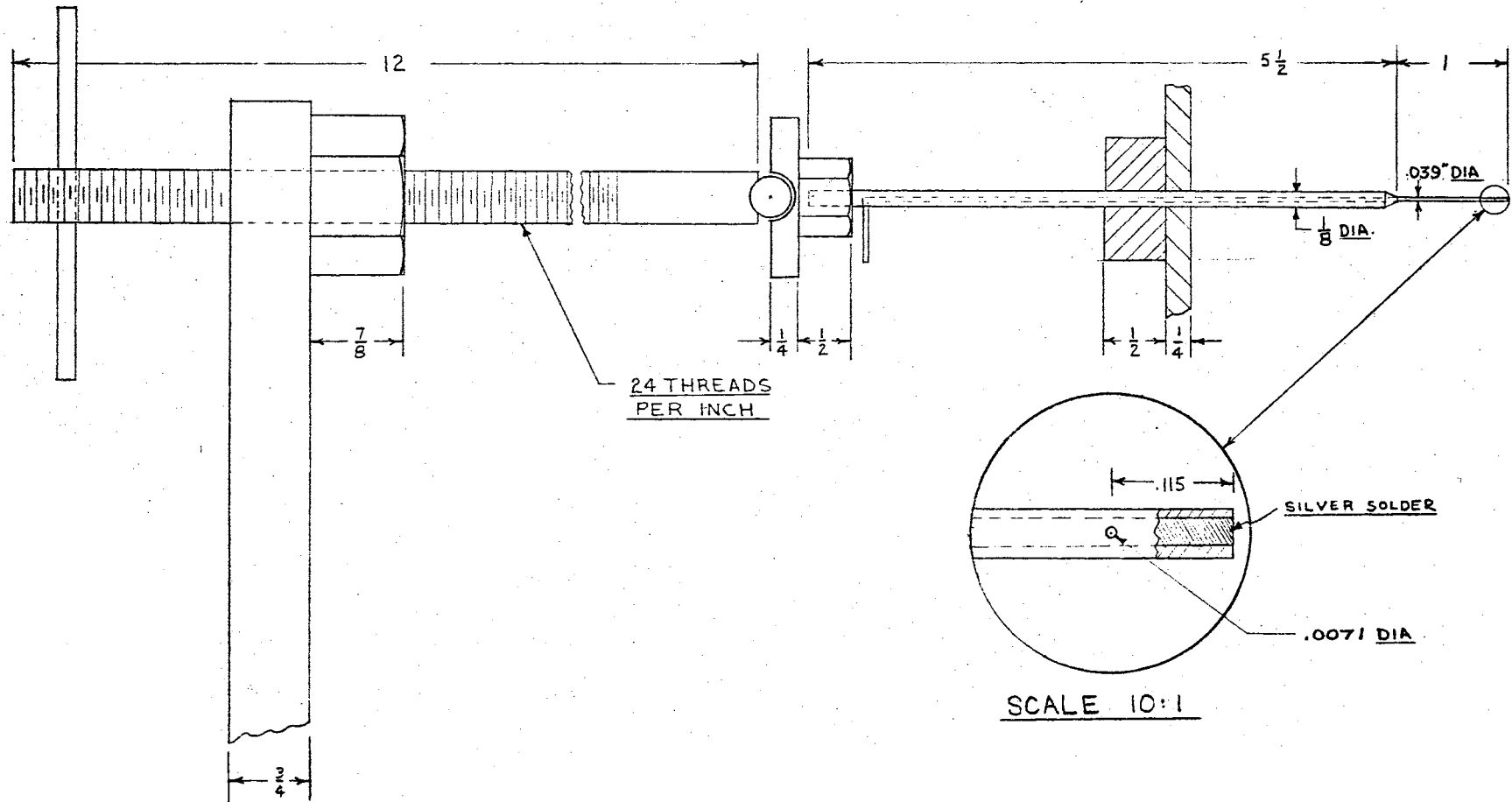
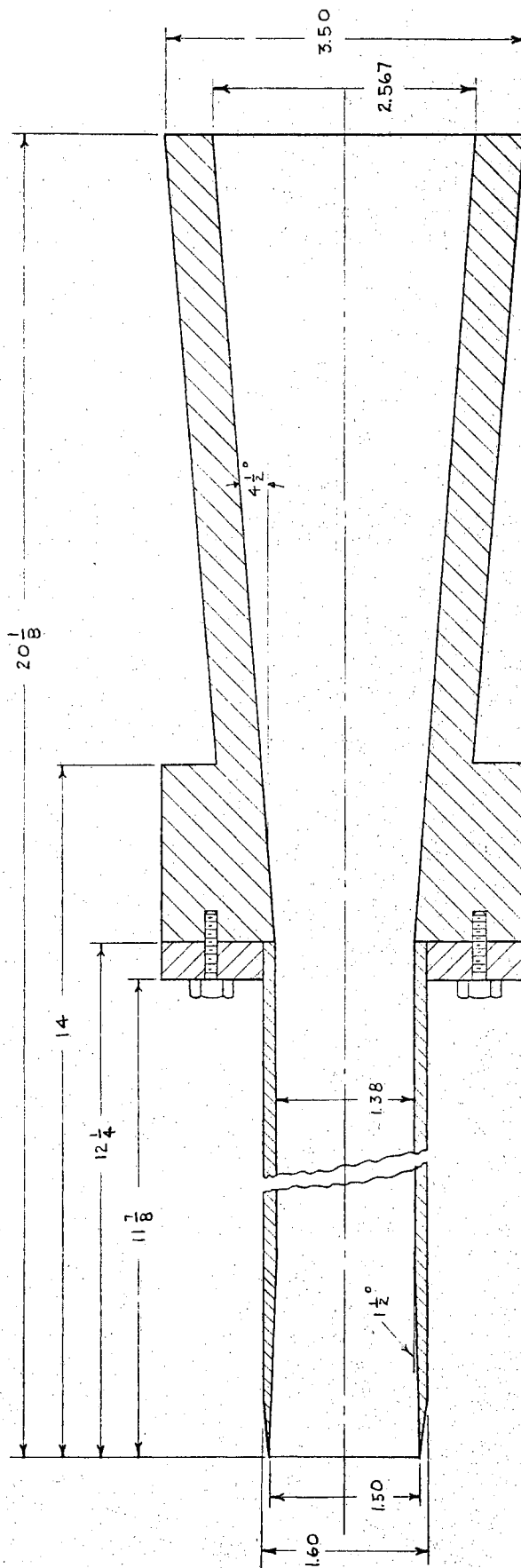


Figure 5.  $\sigma$  Value for Mach Number 3 with Attempted Boundary Layer Correction.

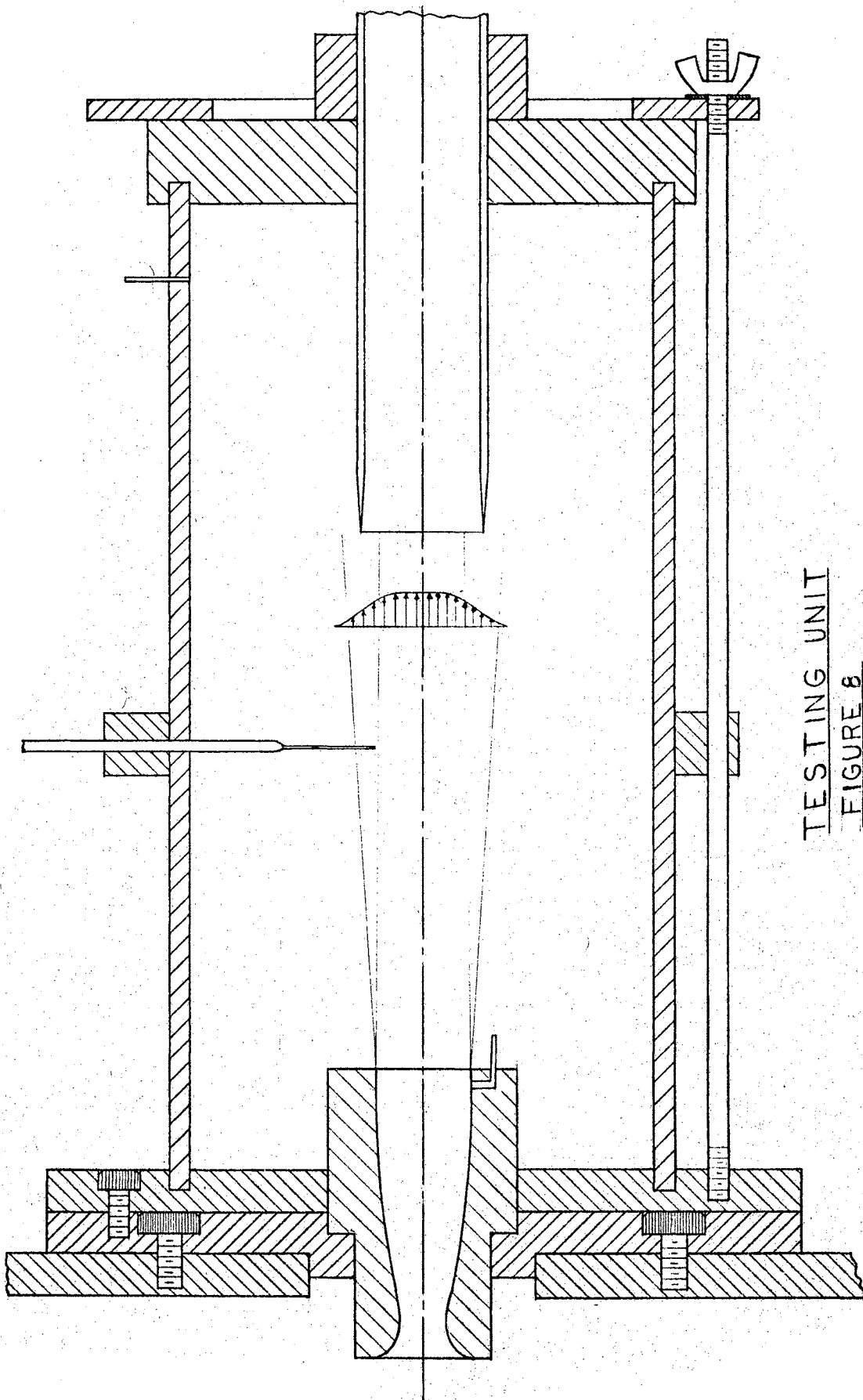
FIGURE 6  
ADVANCING MECHANISM AND PRESSURE PROBE





SUPERSONIC DIFFUSER

FIGURE 7



TESTING UNIT  
FIGURE 8

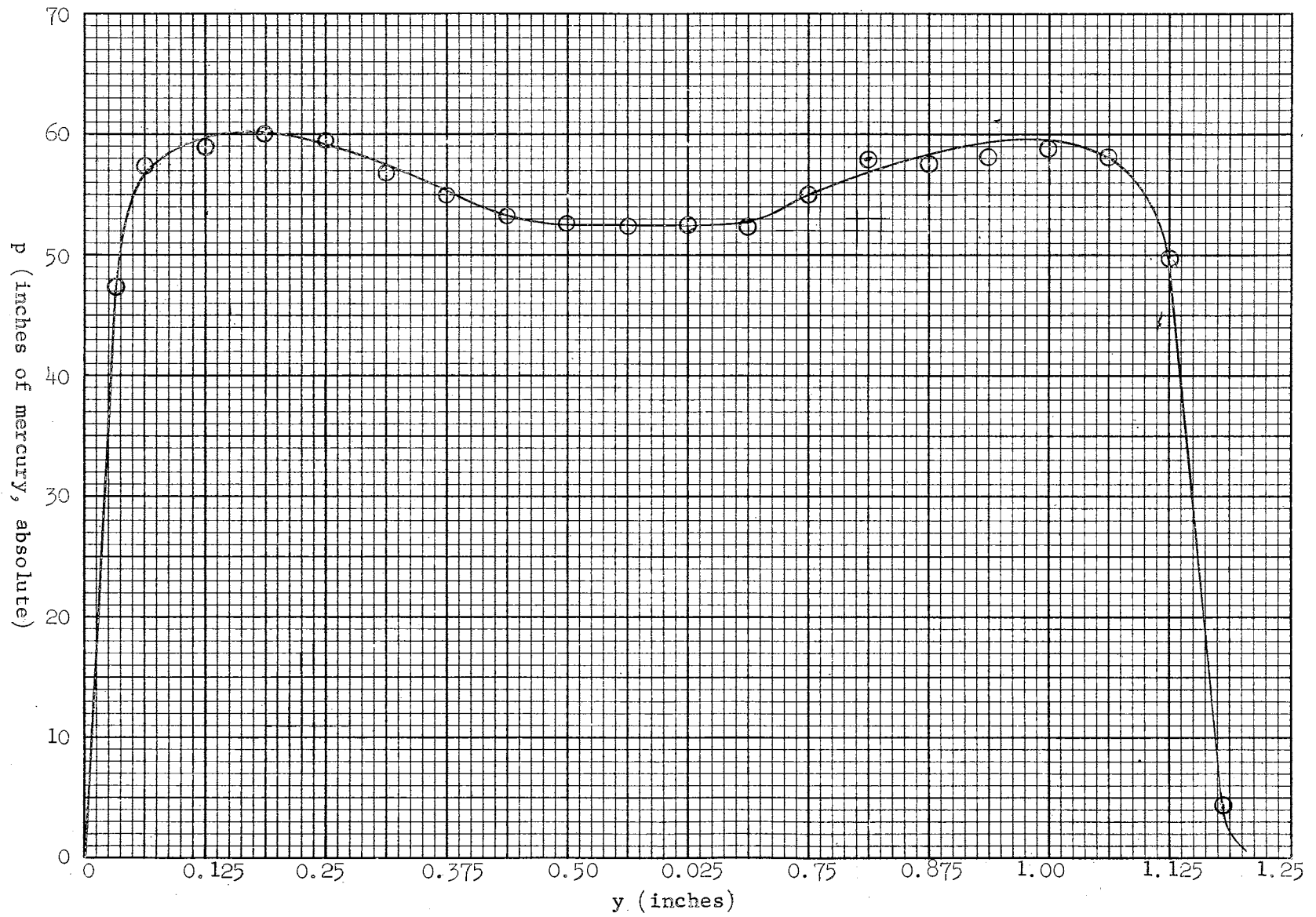


Figure 9. Nozzle Exit Pressure Profile.



Figure 10. Experimental Apparatus



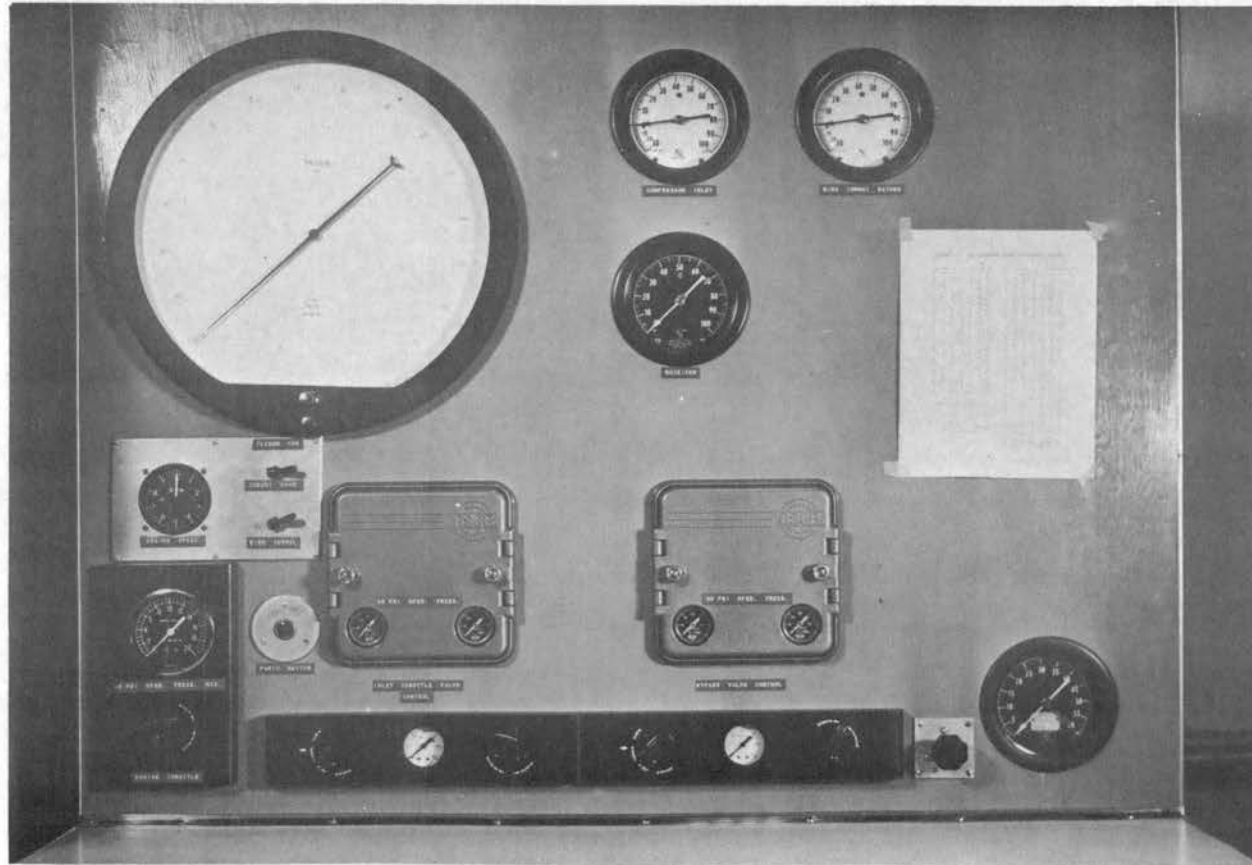


Figure 11. Control Panel

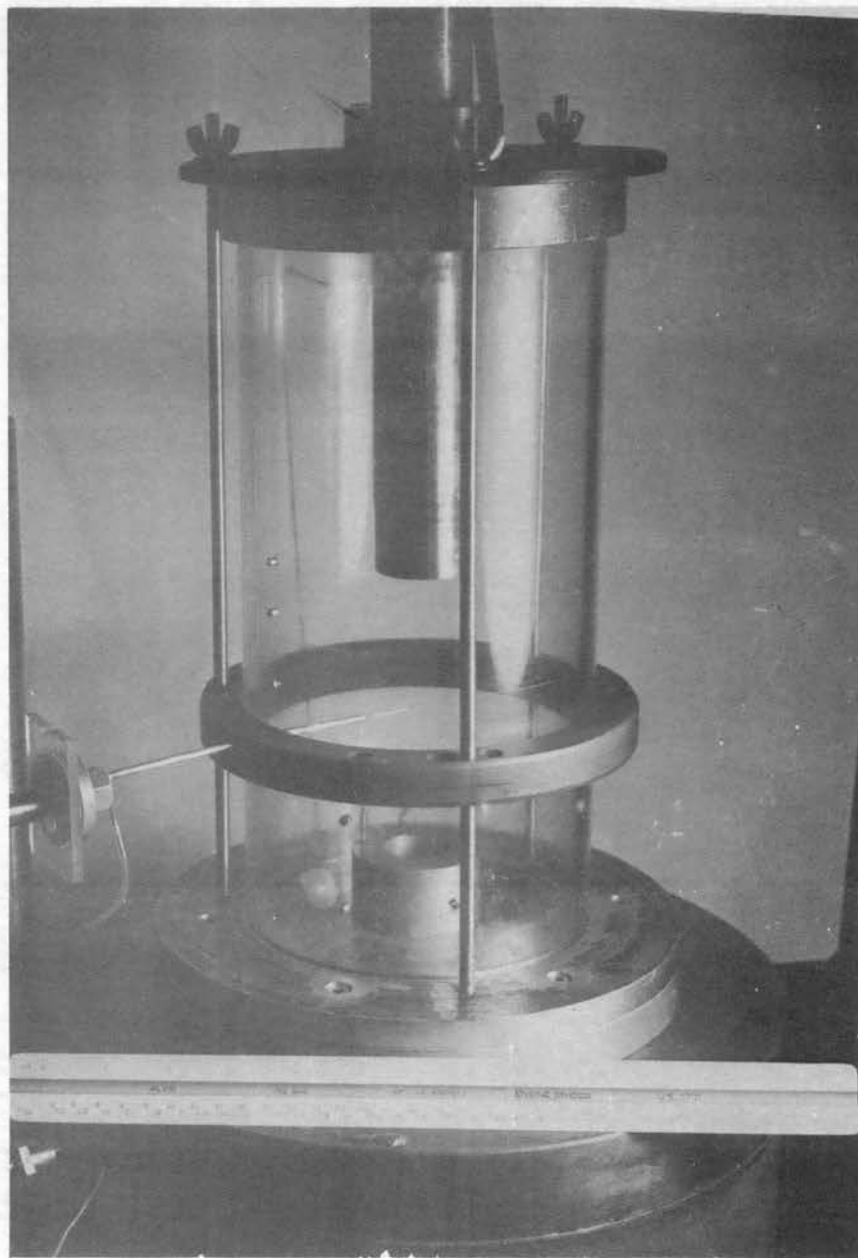


Figure 12. Mixing Chamber

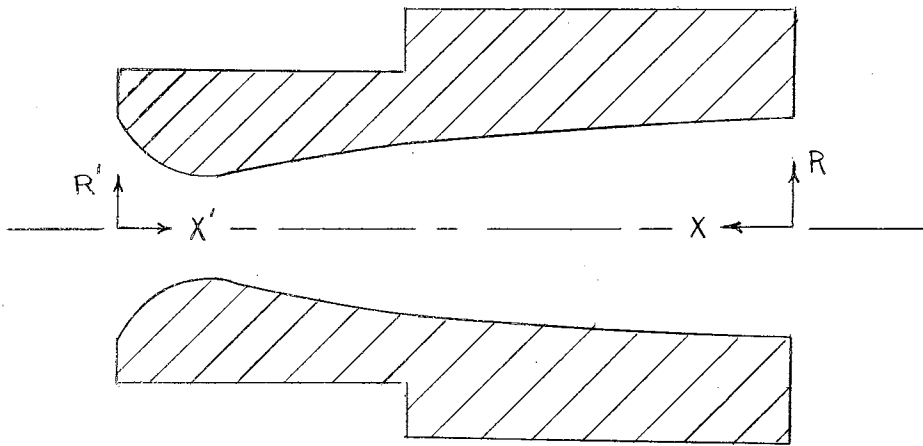
## SELECTED BIBLIOGRAPHY

1. Korst, H. H., Page, R. H., and Childs, M. E., Compressible Two-Dimensional Jet Mixing at Constant Pressure. Univ. of Illinois, ME-TN-392-1, OSR-TN-54-82, Contract No. AF 18(600)392, April 1954.
2. Liepmann, H. W., and Laufer, J. Investigations on Free Turbulent Mixing. NACA TN 1257, 1947.
3. Tollmien, Walter, Calculation of Turbulent Expansion Processes. NACA-TM 1085, 1945.
4. Goertler, H., "Berechnung von Aufgaben der freien Turbulenz auf Grund lines neuen Nherungsansatzes." ZAMM 22, 1942, pp. 244-254.
5. Schlichting, H., Boundary Layer Theory, 4th Edition, McGraw-Hill Book Co., New York, 1960, pp. 590-599.
6. Abramovich, G. N., The Theory of a Free Jet of a Compressible Gas. NACA TM 1058, 1944.
7. Gooderum, P. B., Wood, G. P., and Brevoort, M. J., Investigations with an Interferometer of the Turbulent Mixing of a Free Supersonic Jet. NACA Report 963, 1950.
8. Pai, S. I., "Two-Dimensional Jet Mixing of a Compressible Fluid," Journal of Aeronautical Sciences, Vol. 16, No. 8, 1949, pp. 463-469.
9. University of Maryland, "Optical Study of Two-Dimensional Jet Mixing," Ph.D. Thesis, 1954.
10. Tripp, Wilson, "Analytical and Experimental Investigation of the Base Pressure Behind a Blunt Trailing Edge for Supersonic Two-Dimensional Flow. (Approaching streams have same stagnation temperatures, but different Mach numbers and stagnation pressures.)" Ph.D. Thesis, Univ. of Illinois, June 1956.
11. Goethert, B. H., "Base Flow of Missiles with Cluster-Rocket Exhausts," AF(AS.ARO, Inc.) Aerospace Engineering, March 1961.
12. Foelsch, K., "The Analytic Design of an Axially Symmetric Laval Nozzle for a Parallel and Uniform Jet." Journal of the Aeronautical Sciences, Vol. 16, No. 3, 1949, p. 161.

13. Kline, S. J. "Optimum Design of Straight-Walled Diffusers." ASME Transactions, 1959.
14. Chapman, D. R., Laminar Mixing of a Compressible Fluid, NACA Report 948, 1950.

APPENDIX

NOZZLE CONTOUR DIMENSIONS



X'(inches)	R'(inches)	X(inches)	R(inches)	X(inches)	R(inches)
.0000	0.5778	0.0000	0.5659	2.0196	0.4452
.0041	0.5306	0.1165	0.5623	2.1921	0.4240
.0541	0.4344	0.3198	0.5557	2.3460	0.4017
.1041	0.3849	0.4874	0.5488	2.4838	0.3786
.1541	0.3505	0.6471	0.5408	2.5465	0.3667
.2041	0.3251	0.8168	0.5346	2.6167	0.3546
.2541	0.3060	1.1256	0.5189	2.6403	0.3473
.3041	0.2920	1.3733	0.5023	2.9378	0.2765
.3541	0.2825	1.6145	0.4844	3.0030	0.2750
.4041	0.2769	1.8275	0.4654		
.4541	0.2750				

VITA

Clifford Cleon Chrisman

Candidate for the Degree of

Master of Science

Thesis: EVALUATION OF THE FREE JET SPREADING PARAMETER FOR AXI-SYMMETRIC FLOW OF AIR AT MACH NUMBER THREE

Major Field: Mechanical Engineering (Aeronautical)

Biographical:

Personal Data: Born in Almena, Kansas, September 25, 1934, the son of Cleon C. and Wilma P. Chrisman.

Education: Graduated from East Peoria Community High School, East Peoria, Illinois in 1952; received a Bachelor of Science from Bradley University, with a major in Mechanical Engineering, in June 1956; completed the requirements for Master of Science degree in August 1962.

Professional Experience: Employed by Research Department of Caterpillar Tractor Company June 1956 to November 1956. Entered the United States Air Force in November 1956 and is currently serving on active duty in the grade of First Lieutenant. Attended Aircraft Maintenance Officers School at Chanute AFB from November 1956 to August 1957. Served as a Maintenance Officer in an F-100D tactical fighter squadron in Europe from August 1957 to August 1960.

Honorary Organizations: Pi Mu Epsilon, Sigma Tau

Professional Organizations: American Society of Mechanical Engineers, Society of Automotive Engineers, Institute of Aerospace Sciences.